

# Atom probe microscopy of three-dimensional distribution of silicon isotopes in $^{28}\text{Si}/^{30}\text{Si}$ isotope superlattices with sub-nanometer spatial resolution

Yasuo Shimizu,<sup>1,a)</sup> Yoko Kawamura,<sup>1</sup> Masashi Uematsu,<sup>1,b)</sup> Kohei M. Itoh,<sup>1,c)</sup> Mitsuhiro Tomita,<sup>2</sup> Mikio Sasaki,<sup>3</sup> Hiroshi Uchida,<sup>3</sup> and Mamoru Takahashi<sup>3</sup>

<sup>1</sup>*School of Fundamental Science and Technology, Keio University, 3-14-1 Hiyoshi, Kohoku-ku, Yokohama 223-8522, Japan*

<sup>2</sup>*Corporate Research and Development Center, Toshiba Corporation, 8 Shinsugita-cho, Isogo-ku, Yokohama 235-8522, Japan*

<sup>3</sup>*Toshiba Nanoanalysis Corporation, 1 Komukai Toshiba-cho, Saiwai-ku, Kawasaki 212-8583, Japan*

(Received 4 August 2009; accepted 27 August 2009; published online 8 October 2009)

Laser-assisted atom probe microscopy of 2 nm period  $^{28}\text{Si}/^{30}\text{Si}$  isotope superlattices (SLs) is reported. Three-dimensional distributions of  $^{28}\text{Si}$  and  $^{30}\text{Si}$  stable isotopes are obtained with sub-nanometer spatial resolution. The depth resolution of the present atom probe analysis is much higher than that of secondary ion mass spectrometry (SIMS) even when SIMS is performed with a great care to reduce the artifact due to atomic mixing. Outlook of Si isotope SLs as ideal depth scales for SIMS and three-dimensional position standards for atom probe microscopy is discussed.

© 2009 American Institute of Physics. [doi:10.1063/1.3236673]

High spatial resolution analysis of dopant distribution profiles in silicon (Si) is required for accurate characterization of shallow source/drain (S/D) regions of state-of-the-art Si nanoelectronic devices. Ideally, atomic-scale three-dimensional (3D) mapping is needed for in-depth understanding of the S/D formation processes. Atom probe microscopy is a powerful characterization method to identify mass distributions in materials with the “atomic-scale” spatial resolution.<sup>1–8</sup> Spatially varying compositions in low-resistivity materials were extensively investigated in the early stage of the atom probe microscopy development.<sup>9–13</sup> Especially, the composition, morphology, and abruptness of interfaces were revealed for metal multilayer structures such as Fe/Tb,<sup>10</sup> Cu/Co,<sup>11</sup> CoFe/Cu, CoFe/NiFe,<sup>12</sup> and NiFe/CoFe/Cu/CoFe.<sup>13</sup> The benchmarking results here were the atomic scale visualization of NiFe/CoFe (111) interfaces by atom probe microscopy in both the field-ion imaging and atom probe compositional modes.<sup>12,13</sup> More recently, laser-irradiation during atom probe microscopy has been proven effective for the analysis of highly resistive materials.<sup>14–22</sup> This emergence of the laser-assisted analysis has enabled measurements of 3D distributions of dopants,<sup>17–19</sup> clusters,<sup>20</sup> defects,<sup>21</sup> and impurity segregation<sup>22</sup> in technologically important Si-based materials. The achievement of 3D observation of dopant distributions in state-of-the-art nanoscale device structures was especially of great technological importance,<sup>23</sup> and such directions of research made it clear that reliable methods to overcome the following limitations are needed. Firstly, a sample for atom probe microscopy is

made into a sharp needle with a certain tip curvature, which evolves continuously during the sample evaporation leading to concaving of what is supposed to be a flat plane. Ideally, the standard reconstruction procedure removes the artifact.<sup>24,25</sup> As one needs to fix a number of geometrical parameters (shank angle, initial radius of curvature), a series of buried flat interfaces that do not affect the formation of S/D regions at all might be useful as an internal calibration. Secondly, an absolute 3D length scale is needed. This problem is of no concern once we achieve the atomic resolution of the Si lattices because we can use the lattice image for appropriate image reconstruction and as the length scale. However, achievement of such a technological benchmark requires Si standards that will allow for appropriate image calibration and depth scaling.

The present paper introduces a new concept of Si isotope engineering<sup>26,27</sup> toward establishment of such an ideal standard sample for secondary ion mass spectrometry (SIMS) and atom probe microscopy; Si isotope superlattices (SLs) that are composed of alternating layers of highly enriched  $^{28}\text{Si}$  and  $^{30}\text{Si}$  stable isotopes. Each isotopically enriched layer is only 1 nm thick (7 atomic monolayers) or thinner and it serves as the absolute length scale. The flat interfaces between adjacent  $^{28}\text{Si}$  and  $^{30}\text{Si}$  isotope layers serve as guidelines for appropriate image reconstruction. On the other hand, the mass difference between  $^{28}\text{Si}$  and  $^{30}\text{Si}$  is so small that it hardly affects the Si processing. Therefore, our Si isotope SLs fulfill all the criteria imposed for atom probe microscopy standards.

A detailed description of the growth of Si isotope SLs using solid-source molecular beam epitaxy was given in Refs. 28 and 29. In short, a high resistivity ( $\rho > 2000 \Omega \text{ cm}$ ), 2 in., *n*-type, (100)-oriented floating-zone  $^{\text{nat}}\text{Si}$  ( $^{28}\text{Si}$ : 92.2 at. %,  $^{29}\text{Si}$ : 4.7 at. %, and  $^{30}\text{Si}$ : 3.1 at. %) wafer was employed as a substrate. Subsequently, a  $^{\text{nat}}\text{Si}$  buffer layer of

<sup>a)</sup>Electronic mail: yshimizu@appi.keio.ac.jp. Present address: IMEC vzw, Kapeldreef 75, B-3001 Leuven, Belgium. Also at the Department of Metallurgy and Materials Engineering, K. U. Leuven, B-3001 Leuven, Belgium. JSPS Research Fellow.

<sup>b)</sup>Electronic mail: uematsu@a3.keio.jp.

<sup>c)</sup>Electronic mail: kitoh@appi.keio.ac.jp.

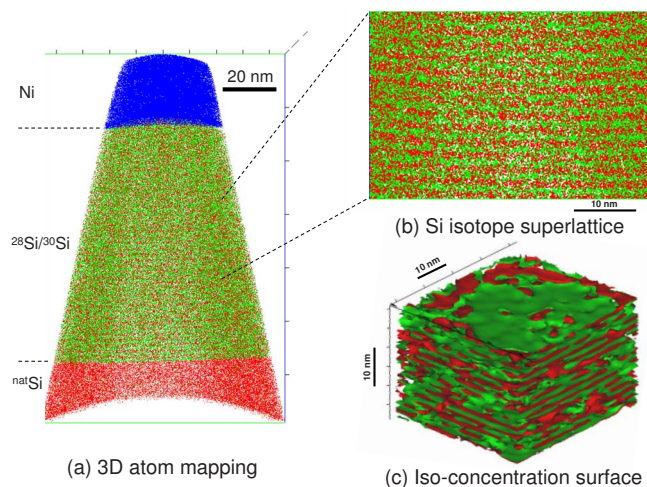


FIG. 1. (Color online) (a) A 3D mapping image of Si isotopes ( $^{28}\text{Si}$  and  $^{30}\text{Si}$ ) in the  $^{28}\text{Si}(1\text{ nm})/^{30}\text{Si}(1\text{ nm})$  isotope SL obtained by atom probe microscopy. The dimension of the reconstructed volume is  $90\text{ nm} \times 90\text{ nm} \times 140\text{ nm}$ . A 30 nm thick of Ni cap layer is seen at the top. Red, green, and blue dots represent  $^{28}\text{Si}$ ,  $^{30}\text{Si}$ , and Ni atoms, respectively. (b) Enlarged view of the part of (a) indicated in the figure. 30 nm in height and 45 nm in side are shown. Only  $\sim 30\%$  of the collected atoms is shown to present the grand view. (c) 3D iso-concentration surface (Threshold:  $2.7 \times 10^{22}\text{ at./cm}^3$ ).

$\sim 100\text{ nm}$  thick was grown at  $750\text{ }^\circ\text{C}$  in order to form a smooth surface followed by the growth of alternating layers of isotopically pure  $^{28}\text{Si}$  and  $^{30}\text{Si}$  at  $650\text{ }^\circ\text{C}$ . The total growth time was approximately 10 h including the growth interruption time between  $^{28}\text{Si}$  and  $^{30}\text{Si}$  layers. Raman spectroscopy of confined optical phonons revealed that the degree of intermixing between adjacent  $^{28}\text{Si}$  and  $^{30}\text{Si}$  layers was approximately 2 atomic monolayers (0.27 nm).<sup>28,29</sup> A commercial laser-assisted local-electrode atom probe microscope (LEAP3000XSi, Imago Scientific Instruments) with a 90 nm flight path and  $<12\text{ ps}$  laser (532 nm) pulse width was employed in this study. The pulse energy and frequency were 0.3 nJ and 500 kHz, respectively. During the analysis, the base temperature of samples was cooled down to  $\sim 50\text{ K}$ . The estimated depth and lateral resolutions were 0.2 and 0.4 nm, respectively,<sup>30</sup> whereas ideal resolutions have been reported recently.<sup>5,8,31,32</sup> The detection efficiency was approximately 50 at. %, which is consistent with the value of 57% on the same LEAP system.<sup>33</sup> A  $\sim 30\text{ nm}$  thick Ni protection layer was deposited on top of the Si isotope SL before shaping of the sample into a needle by Ga focused ion beam.<sup>17,18,34</sup> The  $^{28}\text{Si}$  and  $^{30}\text{Si}$  were resolved clearly in the time-of-flight mass spectrometry as well-separated peak in the counts versus mass spectrum. Lower laser power tends to enhance the intensity of Si having larger positive charges.<sup>35–39</sup> The charge state ratios of  $^{28}\text{Si}^+ / ^{28}\text{Si}^{2+} \sim 0.0090$  and  $^{30}\text{Si}^+ / ^{30}\text{Si}^{2+} \sim 0.0084$  are much smaller than those in the literature even for the nominally same pulse energy of 0.3 nJ,<sup>35</sup> suggesting that in our experiment laser focus and overlap were different compared to the conditions reported by Shariq *et al.*<sup>35</sup> This small laser energy of 0.3 nJ was employed to minimize the sample heating.

Figure 1(a) shows an atom probe microscopy image of the  $^{28}\text{Si}/^{30}\text{Si}$  isotope SL. Alternating layers of Si isotopes were clearly observed along with the  $\sim 30\text{ nm}$  thick Ni cap

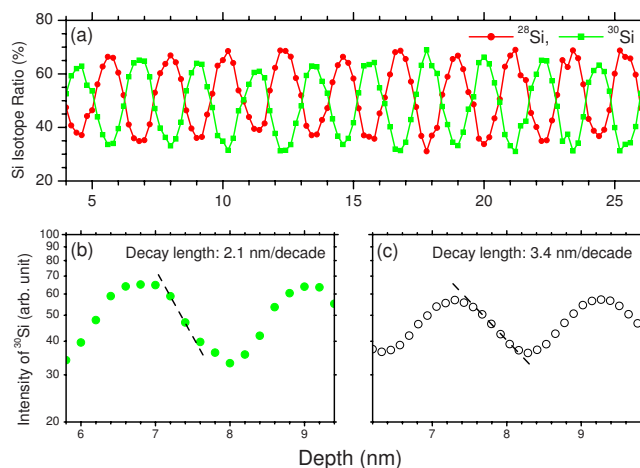


FIG. 2. (Color online) (a) Depth profiles of  $^{28}\text{Si}$  (red) and  $^{30}\text{Si}$  (green) in the  $^{28}\text{Si}(1\text{ nm})/^{30}\text{Si}(1\text{ nm})$  isotope SL along the center of the needle shown in Fig. 1(a). A comparison of the decay lengths of the  $^{30}\text{Si}$  depth profiles between (b) atom probe microscopy and (c) SIMS is shown.

layer at the surface and the  $^{\text{nat}}\text{Si}$  layer in the region deeper than  $\sim 80\text{ nm}$ . Figure 1(b) shows the enlargement of a middle part of the image shown in Fig. 1(a). Atomically flat interfaces of  $^{28}\text{Si}/^{30}\text{Si}$  appear concaved in Fig. 1(b). This artifact comes from the limitation in reconstructing images assuming that the atom emitting surface remains hemispherical through the measurement, where this has been shown not to be the case.<sup>35</sup> Here, the embedded isotope SL structure can be used as the ideal scale to remove this artifact. Figure 1(c) shows the iso-concentration surface of the Si isotope SL in 3D. An important question here is whether one can identify the position of individual isotope with atomic resolution.

In Fig. 2(a), we show the depth profiles of the  $^{28}\text{Si}$  and  $^{30}\text{Si}$  composition along the center of the isotope SL in Fig. 1(a). Here, local compositions within the rectangle cell with dimensions equal to our estimated depth and lateral resolutions of 0.2 nm in height and 0.4 nm in side were plotted with 0.2 nm depth interval. As stated before, our detection efficiency is 50 at. %. Thus, the number of atoms counted within the cell is a half of the number of Si atoms in this region. SIMS measurements (Cameca-SIMS4550) of a sample cut from the same Si isotope SLs were performed with  $\text{O}_2^+$  primary ions accelerated at 150 eV [Fig. 2(c)]. In our case, this condition minimizes the atomic mixing by  $\text{O}_2^+$  bombardment during the SIMS measurements. The decay length by atom probe microscopy estimated in Fig. 2(b) is  $\sim 2.1\text{ nm/decade}$  and this value is much smaller than  $\sim 3.4\text{ nm/decade}$  for SIMS shown in Fig. 2(c). This shows clearly that the spatial resolution of the atom probe is much superior to that of SIMS. Such a comparison between the atom probe and SIMS was previously reported for doping profiles without any absolute depth scale.<sup>40</sup> It is clear that atom probe microscopy of S/D regions formed in Si isotope SLs will lead to simultaneous observation of dopant profiles with absolute depth scale of Si isotopes in the background. It has been shown in Ref. 41 that the abruptness of  $^{28}\text{Si}/^{30}\text{Si}$  interfaces is at most 2 atomic monolayers ( $<0.3\text{ nm}$ ) and, therefore,  $\sim 2.1\text{ nm/decade}$  found in the present atom probe microscopy [Fig. 2(b)] does not appear to be ultimate

resolution. One may need to optimize other conditions such as laser energy, focusing, angle, sample temperature, etc. The present Si isotope SLs will serve as an excellent standard for such optimization processes of the measurement condition and image reconstruction.<sup>33</sup>

Direct imaging of lattice planes perpendicular to  $\langle 100 \rangle$  direction is challenging because of the small interplane separation of  $\sim 0.13$  nm. Therefore, our next plan is to aim for direct observation of lattice plane in  $\langle 111 \rangle$  direction whose lattice spacing is  $\sim 0.32$  nm. Direct lattice plane imaging by atom probe microscopy was previously reported for the (111) NiFe/CoFe interfaces that have interplane spacing of  $\sim 0.2$  nm.<sup>12,13</sup> Combination of the atomic plane resolution and isotopic visualization in atom probe microscopy will allow us to identify the 3D distribution of isotopes with atomic resolution. Such calibrated Si isotope SLs are expected to be the ideal SIMS depth standards<sup>42</sup> and atom probe microscopy length standards.

In conclusion, we have successfully obtained the isotopic distribution in  $^{28}\text{Si}/^{30}\text{Si}$  isotope SL having a 2 nm thick period by laser-assisted atom probe microscopy. The 3D profiling of the stable isotope layers has been obtained with the sub-nanometer spatial resolution. The depth direction spatial resolution by the atom probe microscope was shown to be much better than that by SIMS.

We acknowledge W. Vandervorst (IMEC vzw), T. Kinno (Toshiba Corp.), and R. Ulfig (Imago Scientific Instruments Corp.) for fruitful discussions. This work has been supported in part by Grant-in-Aid for Scientific Research by MEXT (No. 18001002), in part by the Research Program on Collaborative Development of Innovative Seeds by JST, and in part by the Special Coordination Funds for Promoting Science and Technology. Y.S. thanks the Grant-in-Aid for Scientific Research No. 205039 of JSPS and Grant-in-Aid for the Global COE program.

<sup>1</sup>E. W. Müller, J. A. Panitz, and S. B. McLane, *Rev. Sci. Instrum.* **39**, 83 (1968).

<sup>2</sup>D. Blavette, A. Bostel, J. M. Sarrau, B. Deconihout, and A. Menand, *Nature (London)* **363**, 432 (1993).

<sup>3</sup>P. P. Camus, D. J. Larson, and T. F. Kelly, *Appl. Surf. Sci.* **87/88**, 305 (1995).

<sup>4</sup>S. J. Sijbrandij, A. Cerezo, T. J. Godfrey, and G. D. W. Smith, *Appl. Surf. Sci.* **94/95**, 428 (1996).

<sup>5</sup>F. Vurpillot, G. Da Costa, A. Menand, and D. Blavette, *J. Microsc.* **203**, 295 (2001).

<sup>6</sup>K. Hono, *Prog. Mater. Sci.* **47**, 621 (2002).

<sup>7</sup>T. F. Kelly and M. K. Miller, *Rev. Sci. Instrum.* **78**, 031101 (2007).

<sup>8</sup>B. Gault, M. P. Moody, F. de Geuser, D. Haley, L. T. Stephenson, and S. P. Ringer, *Appl. Phys. Lett.* **95**, 034103 (2009).

<sup>9</sup>D. J. Larson, R. L. Martens, and T. F. Kelly, and M. K. Miller, *J. Appl. Phys.* **87**, 5989 (2000).

<sup>10</sup>L. Veiller, F. Danoix, and J. Teillet, *J. Appl. Phys.* **87**, 1379 (2000).

<sup>11</sup>D. J. Larson, D. T. Foord, A. K. Petford-Long, A. Cerezo, and G. D. W. Smith, *Nanotechnology* **10**, 45 (1999).

<sup>12</sup>D. J. Larson, P. H. Clifton, N. Tabat, A. Cerezo, A. K. Petford-Long, R. L. Martens, and T. F. Kelly, *Appl. Phys. Lett.* **77**, 726 (2000).

<sup>13</sup>D. J. Larson, B. D. Wissman, R. L. Martens, R. J. Viellieux, T. F. Kelly, T. G. Gribb, H. F. Erskine, and N. Tabat, *Microsc. Microanal.* **7**, 24 (2001).

<sup>14</sup>G. L. Kellogg and T. T. Tsong, *J. Appl. Phys.* **51**, 1184 (1980).

<sup>15</sup>R. A. King, R. A. D. Mackenzie, G. D. W. Smith, and N. A. Cade, *J. Vac. Sci. Technol. B* **12**, 705 (1994).

<sup>16</sup>B. Gault, F. Vurpillot, A. Vella, M. Gilbert, A. Menand, D. Blavette, and B. Deconihout, *Rev. Sci. Instrum.* **77**, 043705 (2006).

<sup>17</sup>K. Thompson, J. H. Booske, D. J. Larson, and T. F. Kelly, *Appl. Phys. Lett.* **87**, 052108 (2005).

<sup>18</sup>K. Thompson, J. H. Bunton, T. F. Kelly, and D. J. Larson, *J. Vac. Sci. Technol. B* **24**, 421 (2006).

<sup>19</sup>K. Inoue, F. Yano, A. Nishida, T. Tsunomura, T. Toyama, Y. Nagai, and M. Hasegawa, *Appl. Phys. Lett.* **93**, 133507 (2008).

<sup>20</sup>M. Ngamo, S. Duguay, F. Cristiano, K. Daoud-Ketata, and P. Pareige, *J. Appl. Phys.* **105**, 104904 (2009).

<sup>21</sup>K. Thompson, P. L. Flaitz, P. Ronsheim, D. J. Larson, and T. F. Kelly, *Science* **317**, 1370 (2007).

<sup>22</sup>K. Inoue, F. Yano, A. Nishida, T. Tsunomura, T. Toyama, Y. Nagai, and M. Hasegawa, *Appl. Phys. Lett.* **92**, 103506 (2008).

<sup>23</sup>M. Y. Simmons, F. J. Rueß, K.-E. J. Goh, W. Pok, T. Hallam, M. J. Butcher, T. C. G. Reusch, G. Scappucci, A. R. Hamilton, and L. Oberbeck, *Int. J. Nanotechnol.* **5**, 352 (2008).

<sup>24</sup>P. Bas, A. Bostel, B. Deconihout, and D. Blavette, *Appl. Surf. Sci.* **87/88**, 298 (1995).

<sup>25</sup>B. P. Geiser, D. J. Larson, E. Oltman, S. Gerstl, D. Reinhard, T. F. Kelly, and T. J. Prosa, *Microsc. Microanal.* **15**, 292 (2009).

<sup>26</sup>K. Takyu, K. M. Itoh, K. Oka, N. Saito, and V. I. Ozogin, *Jpn. J. Appl. Phys., Part 2* **38**, L1493 (1999).

<sup>27</sup>K. M. Itoh, J. Kato, M. Uemura, A. K. Kaliteevskii, O. N. Godisov, G. G. Devyatych, A. D. Bulanov, A. V. Gusev, I. D. Kovalev, P. G. Sennikov, H.-J. Pohl, N. V. Abrosimov, and H. Riemann, *Jpn. J. Appl. Phys., Part 1* **42**, 6248 (2003).

<sup>28</sup>T. Kojima, R. Nebashi, K. M. Itoh, and Y. Shiraki, *Appl. Phys. Lett.* **83**, 2318 (2003).

<sup>29</sup>Y. Shimizu and K. M. Itoh, *Thin Solid Films* **508**, 160 (2006).

<sup>30</sup>H. Akutsu, H. Itokawa, K. Nakamura, T. Iinuma, K. Suguro, H. Uchida, and M. Tada, *Mater. Res. Soc. Symp. Proc.* **1070**, E02-09 (2008).

<sup>31</sup>T. F. Kelly, B. P. Geiser, and D. J. Larson, *Microsc. Microanal.* **13**, 1604 (2007); <http://dx.doi.org/10.1017/S1431927607077689>.

<sup>32</sup>T. F. Kelly, E. Voelkl, and B. P. Geiser, *Microsc. Microanal.* **15**, 12 (2009).

<sup>33</sup>B. Gault, M. P. Moody, F. de Geuser, G. Tsafnat, A. La Fontaine, L. T. Stephenson, D. Haley, and S. P. Ringer, *J. Appl. Phys.* **105**, 034913 (2009).

<sup>34</sup>D. J. Larson, D. T. Foord, A. K. Petford-Long, H. Liew, M. G. Blamire, A. Cerezo, and G. D. W. Smith, *Ultramicroscopy* **79**, 287 (1999).

<sup>35</sup>A. Shariq, S. Mutas, K. Wedderhoff, C. Klein, H. Hortenbach, S. Teichert, P. Kücher, and S. S. A. Gerstl, *Ultramicroscopy* **109**, 472 (2009).

<sup>36</sup>G. L. Kellogg, *J. Appl. Phys.* **52**, 5320 (1981).

<sup>37</sup>E. A. Marquis and B. Gault, *J. Appl. Phys.* **104**, 084914 (2008).

<sup>38</sup>Y. Zhou, C. Booth-Morrison, and D. N. Seidman, *Microsc. Microanal.* **14**, 571 (2008).

<sup>39</sup>D. R. Kingham, *Surf. Sci.* **116**, 273 (1982).

<sup>40</sup>P. Ronsheim, P. Flaitz, M. Hatzistergos, C. Molella, K. Thompson, and R. Alvis, *Appl. Surf. Sci.* **255**, 1547 (2008).

<sup>41</sup>Y. Shimizu, M. Uematsu, and K. M. Itoh, *Phys. Rev. Lett.* **98**, 095901 (2007).

<sup>42</sup>Y. Shimizu, A. Takano, and K. M. Itoh, *Appl. Surf. Sci.* **255**, 1345 (2008).